



Mast cells protect from post-traumatic spinal cord damage in mice by degrading inflammation-associated cytokines via mouse mast cell protease 4[☆]



Sofie Nelissen^{a,1}, Tim Vanganswinkel^{a,1}, Nathalie Geurts^a, Lies Geboes^a, Evi Lemmens^a, Pia M. Vidal^a, Stefanie Lemmens^a, Leen Willems^a, Francesco Boato^{a,2}, Dearbhaile Dooley^a, Debora Pehl^b, Gunnar Pejler^c, Marcus Maurer^b, Martin Metz^b, Sven Hendrix^{a,*}

^a Dept. of Morphology & Biomedical Research Institute, Hasselt University, Diepenbeek, Belgium

^b Dept. of Dermatology and Allergy, Allergie-Centrum-Charité, Charité-Universitätsmedizin Berlin, Germany

^c Dept. of Anatomy, Physiology and Biochemistry, Swedish University of Agricultural Sciences, Uppsala, Sweden

ARTICLE INFO

Article history:

Received 12 January 2013

Revised 23 August 2013

Accepted 17 September 2013

Available online 26 September 2013

Keywords:

mMCP4

Mast cell

Inflammation

Spinal cord injury

MCP-1

TNF- α

IL-6

IL-10

IL-13

ABSTRACT

Mast cells (MCs) are found abundantly in the central nervous system and play a complex role in neuroinflammatory diseases such as multiple sclerosis and stroke. In the present study, we show that MC-deficient *Ki^{W-sh/W-sh}* mice display significantly increased astrogliosis and T cell infiltration as well as significantly reduced functional recovery after spinal cord injury compared to wildtype mice. In addition, MC-deficient mice show significantly increased levels of MCP-1, TNF- α , IL-10 and IL-13 protein levels in the spinal cord. Mice deficient in mouse mast cell protease 4 (mMCP4), an MC-specific chymase, also showed increased MCP-1, IL-6 and IL-13 protein levels in spinal cord samples and a decreased functional outcome after spinal cord injury. A degradation assay using supernatant from MCs derived from either mMCP4^{-/-} mice or controls revealed that mMCP4 cleaves MCP-1, IL-6, and IL-13 suggesting a protective role for MC proteases in neuroinflammation. These data show for the first time that MCs may be protective after spinal cord injury and that they may reduce CNS damage by degrading inflammation-associated cytokines via the MC-specific chymase mMCP4.

© 2013 The Authors. Published by Elsevier Inc. All rights reserved.

Introduction

Mast cells (MCs) are abundant at host/environment interfaces, i.e. the skin, airways and gut, where they are known to contribute significantly to the induction of inflammation in the context of allergic reactions and innate immune responses to pathogens (Henz et al., 2001; Marshall,

2004). In the mammalian central nervous system (CNS), MCs are reported as being mainly located in the leptomeninges, the dura mater, the choroid plexus and the parenchyma of the thalamic–hypothalamic region, where they are generally found along the blood vessels (Zappulla et al., 2002). MCs in the healthy brain of rats are found mostly in the thalamus (Brenner et al., 1994), where they are thought to contribute to sensory processing, blood vessel permeability and local hemodynamics (Kil et al., 1999). MC-derived histamine has been reported to potentiate synaptically mediated excitotoxicity in hippocampal neurons of mice in vitro (Skaper et al., 2001) and MC activation reportedly promotes delayed neurodegeneration in murine mixed neuron–glia hippocampal cultures (Skaper et al., 1996).

Substantial progress has been made over the last decade in elucidating the crucial role of MCs in inflammatory CNS disorders such as multiple sclerosis (MS) and stroke [reviewed in Nelissen et al., 2013]. In the animal model of human MS, experimental autoimmune encephalomyelitis (EAE), sites of inflammatory demyelination in the CNS are characterized by MC accumulation and the percentage of degranulated MCs in the CNS correlates with the clinical onset of disease symptoms (Brenner et al., 1994). Furthermore, it has been demonstrated that MC-deficient *W/W^v* mice suffer from a significantly

Abbreviations: MCs, mast cells; MS, multiple sclerosis; EAE, experimental autoimmune encephalomyelitis; WT, wildtype; SCI, spinal cord injury; mMCP4, mouse mast cell protease 4; BMS, basso mouse scale; GFAP, glial fibrillary acidic protein; MBP, myelin basic protein; Iba-1, ionized calcium binding adaptor molecule 1; RT, room temperature; SN, supernatants; BMCMCs, bone marrow-derived cultured mast cells; IL, interleukin; TNF- α , tumor necrosis factor α ; MCP-1, monocyte chemoattractant protein 1.

[☆] This is an open-access article distributed under the terms of the Creative Commons Attribution License, which permits unrestricted use, distribution, and reproduction in any medium, provided the original author and source are credited.

* Corresponding author at: Dept. of Morphology & Biomedical Research Institute, Martelarenlaan 42, Hasselt, Diepenbeek 3500, Belgium. Fax: +32 11 26 9299.

E-mail address: sven.hendrix@uhasselt.be (S. Hendrix).

Available online on ScienceDirect (www.sciencedirect.com).

¹ SN and TV contributed equally to this study.

² Present address: Université Pierre et Marie Curie, Institut de la Vision, Paris, France.

less severe myelin-oligodendrocyte-glycoprotein-induced EAE and restoration of the MC population with wildtype (WT) MCs results in disease severity similar to WT mice (Brown et al., 2002; Robbie-Ryan et al., 2003; Secor et al., 2000; Tanzola et al., 2003). In contrast to these previous studies, other data revealed that MCs may be dispensable for EAE development (Bennett et al., 2009; Feyerabend et al., 2011). Conversely, it has been shown that *Kit^{W-sh/W-sh}* mice develop more severe EAE, which is characterized by earlier onset, more severe paralysis, and more extensive demyelination and inflammatory infiltration (Li et al., 2011). MCs are also critically involved in the pathophysiology of ischemic stroke (Lindsberg et al., 2010; Strbian et al., 2009). MCs are one of the first cells to respond to hypoxic-ischemic brain damage in the immature brain. Inhibition of the early MC response resulted in significant neuroprotection (Jin et al., 2009). In the adult rat, MCs are involved in ischemic brain edema early after focal cerebral ischemia onset (Strbian et al., 2006). In the model of intracerebral hemorrhage, MC-deficient rats responded with significantly better neurologic scores than WT animals (Strbian et al., 2007).

In the present study we have analyzed the effects of MC-deficiency in a mouse model of spinal cord injury (SCI). In addition, we propose here a potential new mechanism in which MCs and their secreted protease mMCP4 exert protective effects after CNS trauma by degrading inflammation-associated cytokines.

Materials and methods

Animals

All experiments were performed using 9- to 11-week-old C57BL/6 mice (Harlan, the Netherlands or The Jackson Laboratory, USA), MC-deficient *W-sash* c-kit mutant knockout mice (*Kit^{W-sh/W-sh}*) (Grimbaldeston et al., 2005) (Jackson Laboratory, USA) and mMCP4-deficient (*mMCP4^{-/-}*) mice (Tchougounova et al., 2003) that were housed in a conventional animal facility at Hasselt University under regular conditions, i.e. in a temperature-controlled room (20 ± 3 °C) on a 12 h light–dark schedule and with food and water ad libitum; all experiments were approved by the local ethical committee of Hasselt University and were performed according to the guidelines described in Directive 2010/63/EU on the protection of animals used for scientific purposes.

Spinal cord T-cut hemisection injury

T-cut hemisection injury was performed as described before (Loske et al., 2012; Tuszyński and Steward, 2012). Briefly, 9- to 11-week-old anesthetized female mice underwent a partial laminectomy at thoracic level T8. For the spinal cord bilateral hemisection, iridectomy scissors were used to transect left and right dorsal funiculus, the dorsal horns and additionally the ventral funiculus (T-cut (Loske et al., 2012)). It is important to note that this “T-cut” procedure results in a complete transection of the dorsomedial and ventral corticospinal tract (CST) and impairs several other descending and ascending tracts. The muscles were sutured and the back skin closed with wound clips.

Locomotion tests

Starting 1 day after surgery, functional recovery in SCI mice was measured for three weeks according to the Basso Mouse Scale (BMS) (Basso et al., 2006). The BMS is a 10-point locomotor rating scale (9 = normal locomotion; 0 = complete hind limb paralysis), in which mice are scored by two investigators blinded to the experimental groups, and which is based on hind limb movements made in an open field during a 4-min interval. Data shown represent mean values per experimental group \pm SEM.

Immunohistochemical analysis of the spinal cord

Spinal cord cryosections (10 μ m) obtained from animals transcardially perfused 21 days after surgery with ringer solution containing heparin, followed by 4% paraformaldehyde, were preincubated with 10% normal goat serum in PBS containing 5% Triton X-100 for 30 min at room temperature (RT). The following primary antibodies were then incubated for 2 h at RT: rat anti-CD4 (1:500; BD biosciences, Belgium), mouse anti-glial fibrillary acidic protein (GFAP) (1:500; Sigma-Aldrich, Belgium), rabbit anti-myelin basic protein (MBP) (1:100; Millipore, Belgium) and rabbit anti-ionized calcium binding adaptor molecule 1 (Iba-1) (1:350; Wako, Germany).

Following repeated washing steps with PBS, secondary antibodies were applied for 1 h at RT. These were goat anti-rat Alexa Fluor 568, goat anti-mouse Alexa Fluor 568 and goat anti-rabbit Alexa Fluor 488 (dilution 1:250; Invitrogen, Belgium), respectively. After removal of unbound antibodies, DAPI counterstaining was performed for 10 min and sections were mounted. For measurement of lesion size, astrogliosis and inflammatory infiltrate, 5 to 6 sections per animal (8 animals per group) containing the lesion center were analyzed, as described (Loske et al., 2012). Lesion size was evaluated using anti-GFAP immunofluorescence, while the demyelinated area was evaluated using anti-MBP immunofluorescence. The T helper cell infiltration was evaluated by double staining against CD4 and Iba-1 in order to exclude CD4 + microglial cells. Quantification of GFAP and Iba-1 expression was performed by intensity analysis using ImageJ open source software (NIH) within rectangular areas of 100 μ m \times 100 μ m extending from 600 μ m cranial to 600 μ m caudal from the lesion epicenter. The infiltration of T helper cells was determined by quantifying all T helper cells in the entire perilesional area, 5 mm distal and proximal from the lesion center. For standardization, the analyses were performed on 7 spinal cord sections (per mice) representing the perilesional area, i.e. the lesion epicenter as well as consecutive caudal and cranial sections.

Real-time PCR

Cytokine/chemokine mRNA levels were investigated in different phases after SCI, namely the acute phase (1 h, 6 h, 2 days), the first T cell peak (4 days), the first peak of microglia activation (7 days), the second peak of immune activation (14 and 21 days) and finally at the early stage of the chronic remodeling phase (28 days) (Beck et al., 2010). RNA was isolated from spinal cords of uninjured mice, sham-operated animals and animals with dorsal T-cut hemisection using the RNeasy Mini Plus Kit (Qiagen, the Netherlands), according to the manufacturer's instructions. After reverse transcription (Promega, the Netherlands), cDNAs were amplified by means of specific commercially available primers for interleukin (IL)-1 β , IL-4, IL-6, IL-10, IL-13, tumor necrosis factor α (TNF- α) and monocyte chemoattractant protein 1 (MCP-1) (Taqman Gene Expression Assays) on a ABI PRISM 7500 sequence detection system (Applied Biosystems, USA). Briefly, amplification conditions consisted of an initial denaturing/activation step at 95 °C for 20 s, followed by 40 cycles of 3 s at 95 °C and 30 s at 60 °C. A threshold cycle was calculated and relative quantification was obtained by comparison with the threshold cycle obtained by amplifying samples with the reference housekeeping genes β -actin-, hypoxanthine guanine phosphoribosyl transferase 1 and β -glucuronidase. Only statistically significant differences were shown in the figures. If there were no significant differences, findings were reported as “data not shown”.

Protein expression in spinal cord and serum samples

Cytokine/chemokine protein levels (systemic and local) were investigated in different phases after SCI (see Real time-PCR). To determine IL-4, IL-6, IL-10, IL-13, MCP-1 and TNF- α protein levels in spinal cord and serum samples from C57BL/6 mice, MC-deficient *Kit^{W-sh/W-sh}* mice and mMCP4^{-/-} mice (3 groups: uninjured mice, sham-operated mice

(only laminectomy) and operated mice with dorsal hemisection), animals were sacrificed at selected time points (1 and 6 h, 2, 4, 7, 14, 21 and 28 days post injury). At these time points, mice were overdosed with Nembutal, serum samples were taken via cardiac puncture, before the mice were transcardially perfused with ringer solution containing heparin. After perfusion, spinal cord tissue was collected in a precisely standardized region (0.5 cm proximal to 0.5 cm distal of the T-cut). Standardized tissue samples were homogenized with a disposable pestle (VWR, Belgium) by adding Procarta lysis buffer, containing protease inhibitors (Panomics, Italy). Cell lysates were centrifuged at 10000 RPM for 10 min and supernatants (SN) were stored at -20°C until measurement. Protein levels were quantitatively determined in serum samples and in the SN of spinal cord homogenates by flow cytometry analysis using the Cytometric Bead Array Mouse Flex set system (BD biosciences) according to the manufacturer's instructions. Since cytokine levels in uninjured WT mice are different compared to cytokine levels in uninjured mMCP4 $^{-/-}$ mice, we decided to express these cytokine levels as a ratio of injured to uninjured mice for WT mice and mMCP4 $^{-/-}$ mice. To calculate the ratio we had to avoid the mathematical problem to divide by zero (0), therefore, in samples with undetectable levels of cytokines, values were arbitrarily defined as 1. Briefly, serial dilutions (1/2 v/v) of the standard were prepared. The samples were incubated with capture beads at RT for 1 h. After the incubation, detection beads were added and samples were incubated for another hour at RT. Finally, all samples were washed with wash buffer. Analysis was performed using FACSArray Bioanalyzer and FCAP software (BD biosciences). Only statistically significant differences were shown in the figures. If there were no significant differences, findings were reported as "data not shown". Data represent mean values \pm SEM.

Bone marrow-derived cultured mast cells (BMCs)

Murine BMCs were obtained, as described (Dudeck et al., 2010), by culturing primary bone marrow cells isolated from the femurs of C57BL/6 mice and of mMCP4 $^{-/-}$ mice in IMDM with L-glutamine (Invitrogen) supplemented by 10% FCS (Biocrom AG, Germany), 1% penicillin/streptomycin (Invitrogen), 0.002% alpha-monothio glycerol (Sigma-Aldrich) supplemented with 10 ng/ml recombinant mouse IL-3 (Invitrogen). BMC cultures were used after 4 weeks and consisted of \pm 95% MCs as controlled by surface expression of Fc-epsilon receptor 1 (eBioscience, USA) by flow cytometry analysis (data not shown).

Degranulation assay

To obtain SN for the degradation assay, a degranulation assay was performed. Degranulation of BMCs was measured by using the β -hexosaminidase assay. Mature BMCs were collected (5×10^4 cells), washed and stimulated for 30 min at 37°C and 5% CO_2 by 1 μM ionomycin (Sigma-Aldrich) in 100 μl Tyrode's buffer (130 mM NaCl, 5 mM KCl, 1 mM MgCl_2 , 1.4 mM CaCl_2 , 10 mM Hepes, 5.6 mM glucose and 0.01% BSA in MilliQ). SN was then collected and used for the degradation assay. Twenty-five microliters of the SN was used for the enzymatic reaction. The cell pellets were lysed using 1% Triton X-100 for 5 min at RT and another 25 μl SN was collected. Next, 25 μl of 4 mM 4-Nitrophenyl N-acetyl- β -D-glucosaminide (Sigma-Aldrich) (in a 0.2 M Na_2HPO_4 and 0.4 M citric acid solution buffer [pH 4.5]) was added to the SN followed by an incubation for 1 h at 37°C . The reaction was terminated by the addition of 150 μl 200 mM glycine buffer (pH 7.0) and absorbance (OD) was measured using a plate reader at a wavelength of 405 nm. The degranulation ratio was calculated using the following formula: $[\text{OD SN} / \text{OD (SN cell lysate)}] \times 10$.

Degradation assay

Murine recombinant IL-1 β , IL-4, IL-6, IL-10, IL-13, TNF- α and MCP-1 (400 ng) (Tebu-bio, Belgium) were incubated for 6, 48, or 96 h at 37°C

in 20 μl MilliQ or in 4 μl MilliQ with 16 μl supernatant from BMCs derived from either C57BL/6 or from mMCP4 $^{-/-}$ mice. The samples were mixed with Novex® Tricine SDS Sample buffer and NUPAGE® Reducing Agent (Invitrogen) and the cleaved fragments were identified using tris-tricine SDS-PAGE on 10% Novex® Tricine Gels and a SilverXpress® Silver Staining Kit (Invitrogen). The quantification of the bands was performed by intensity analysis using ImageJ.

Statistical analysis

Locomotion tests as well as histological evaluation of the astrocyte and microglia/macrophage reaction were analyzed using two-way ANOVA for repeated measurements with the Bonferroni correction for multiple comparisons. All other differences between two groups were evaluated using the nonparametric Mann–Whitney U-test. The analyses were performed using Prism 5.0 software (GraphPad Software, San Diego, CA, USA). Differences were considered statistically significant when $p < 0.05$.

Results

MC-deficiency results in increased T cell infiltration, astrogliosis and functional impairment after SCI

When we subjected MC-deficient $\text{Kit}^{\text{W-sh/W-sh}}$ mice and their control C57BL/6 mice (further referred to as WT mice) to a dorsal T-cut hemisection and monitored functional recovery using the BMS, we found that locomotor function was significantly decreased from day 7 onwards in MC-deficient $\text{Kit}^{\text{W-sh/W-sh}}$ mice compared to WT mice (Fig. 1A). Similar results were also obtained in $\text{Kit}^{\text{W/KitW-v}}$ mice (data not shown). The lesion size (Figs. 1B, C, F) and the demyelinated area (Figs. 1D, E, G) were determined by immunofluorescence for GFAP and MBP followed by image analysis with ImageJ. The evaluation of the lesion size by GFAP immunofluorescence revealed a slight, non-significant trend towards an increased lesion size in the MC-deficient $\text{Kit}^{\text{W-sh/W-sh}}$ mice compared to WT mice, 3 weeks after SCI. By measuring the GFAP intensity just below the lesion, 600 μm caudal and 600 μm cranial, in squares of 100 μm to 100 μm (Fig. 1H), astrogliosis was evaluated. GFAP expression peaked in both WT and MC-deficient $\text{Kit}^{\text{W-sh/W-sh}}$ mice around the lesion epicenter and decreased further caudal and cranial from the lesion epicenter (Fig. 1I). At 3 weeks after SCI, GFAP expression levels were slightly but significantly higher in MC-deficient mice compared to control mice ($p < 0.001$), indicating an increased astrocyte reaction after SCI in MC-deficient $\text{Kit}^{\text{W-sh/W-sh}}$ mice compared to WT mice. To investigate the inflammatory response after SCI, immunofluorescence for the macrophage/microglia marker Iba-1 (Figs. 2A–C) and the T helper cell marker CD4 (Figs. 2D–F) was performed on spinal cord sections. No difference in the microglia/macrophage reaction between WT and MC-deficient $\text{Kit}^{\text{W-sh/W-sh}}$ mice, 3 weeks after SCI, was observed. At 3 weeks after SCI, a significant increase in the mean number of T cells per 6 spinal cord sections in the MC-deficient $\text{Kit}^{\text{W-sh/W-sh}}$ mice, compared to WT mice, could be observed (Fig. 2D, $p < 0.05$).

Peak mRNA and protein levels of inflammation-associated cytokines in the acute phase after SCI

To test the hypothesis that MCs may restrict inflammatory processes and degeneration after CNS trauma, we first analyzed cytokine/chemokine mRNA (local) and protein levels (systemic and local) in different phases after SCI.

In line with previous findings by others (Bartholdi and Schwab, 1997; Pan et al., 2002; Pineau and Lacroix, 2007; Streit et al., 1998), TNF- α mRNA levels significantly increased within 1 h after SCI compared to mRNA levels in the uninjured and laminectomy (sham) mice (Fig. 3C). This was also true for IL-10 mRNA levels (Fig. 3D). Peak mRNA levels of IL-6 (Fig. 3A), IL-1 β (Fig. 3E) and the chemokine MCP-1 (Fig. 3B) were observed 6 h after SCI. In contrast to previous findings

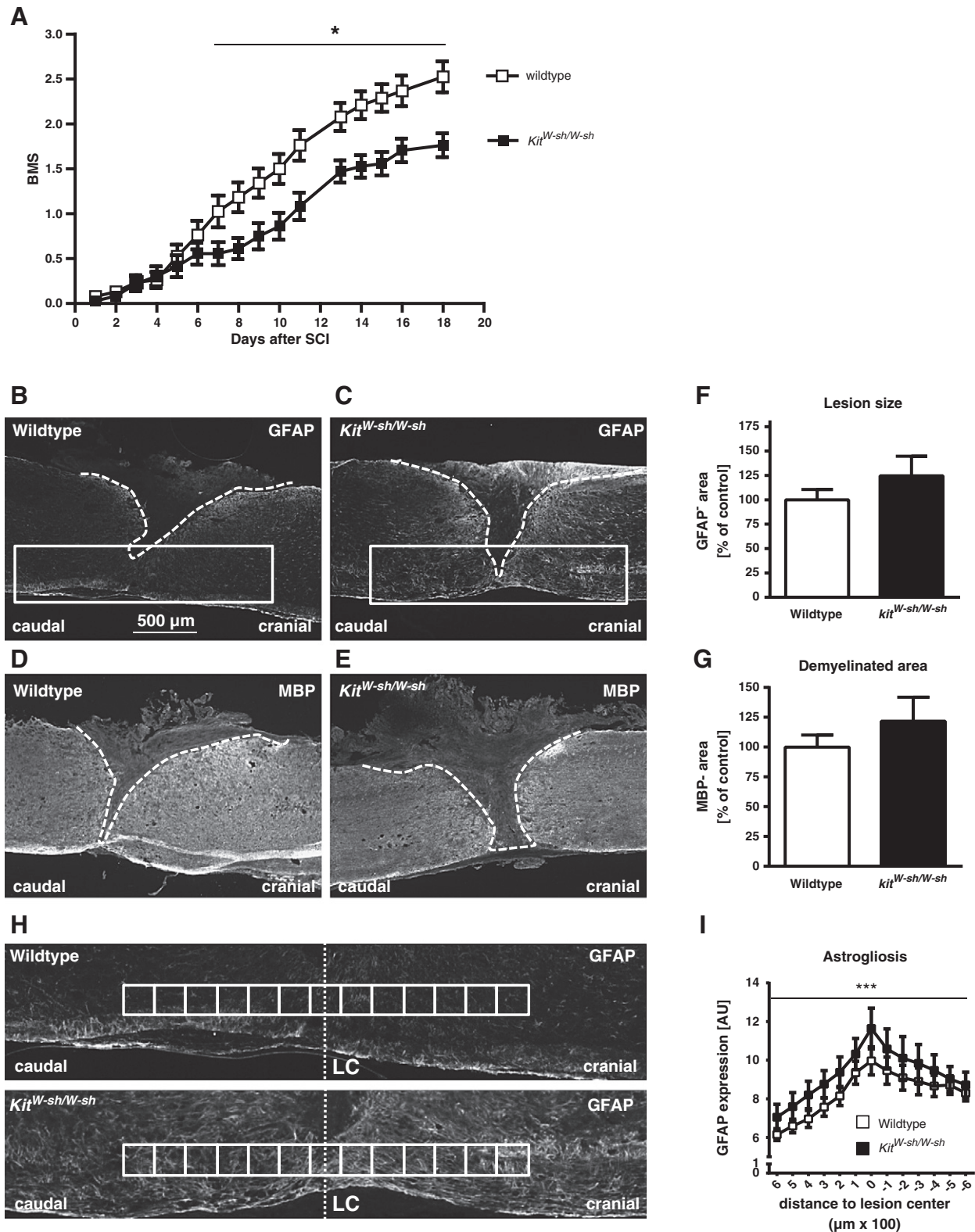


Fig. 1. Decreased functional outcome and increased perilesional astrogliosis in MC-deficient *Kit^{W-sh/W-sh}* mice compared to WT after SCI. MC-deficiency in *Kit^{W-sh/W-sh}* mice results in a significantly decreased BMS score after SCI (A). * $p < 0.05$, $n = 18$ –19/group. Two independent experiments. Representative photomicrographs of spinal cord sections including the injury epicenter, of WT mice (B, D) and MC-deficient *Kit^{W-sh/W-sh}* mice (C, E). Sections were stained for GFAP (B, C) and MBP (D, E) to determine the lesion size (F) and the demyelinated area (G). Boxed regions in B and C are shown in H. Quantification of astrogliosis after SCI was performed by intensity analysis of GFAP staining within square areas of $100 \mu\text{m} \times 100 \mu\text{m}$ (white boxes) just below the lesion site (delineated, with a vertical dotted line representing the lesion epicenter [LC]), extending from $600 \mu\text{m}$ cranial to $600 \mu\text{m}$ caudal from the lesion epicenter (H). Image analysis revealed a significantly increased astrocytic reaction in the MC-deficient mice after SCI, compared to WT mice (I). Scale bars: B–E = $500 \mu\text{m}$. Data represent mean \pm SEM (expressed as percentage of control in panel F and G). *** $p < 0.001$, $n = 8$ /group. Two independent experiments.

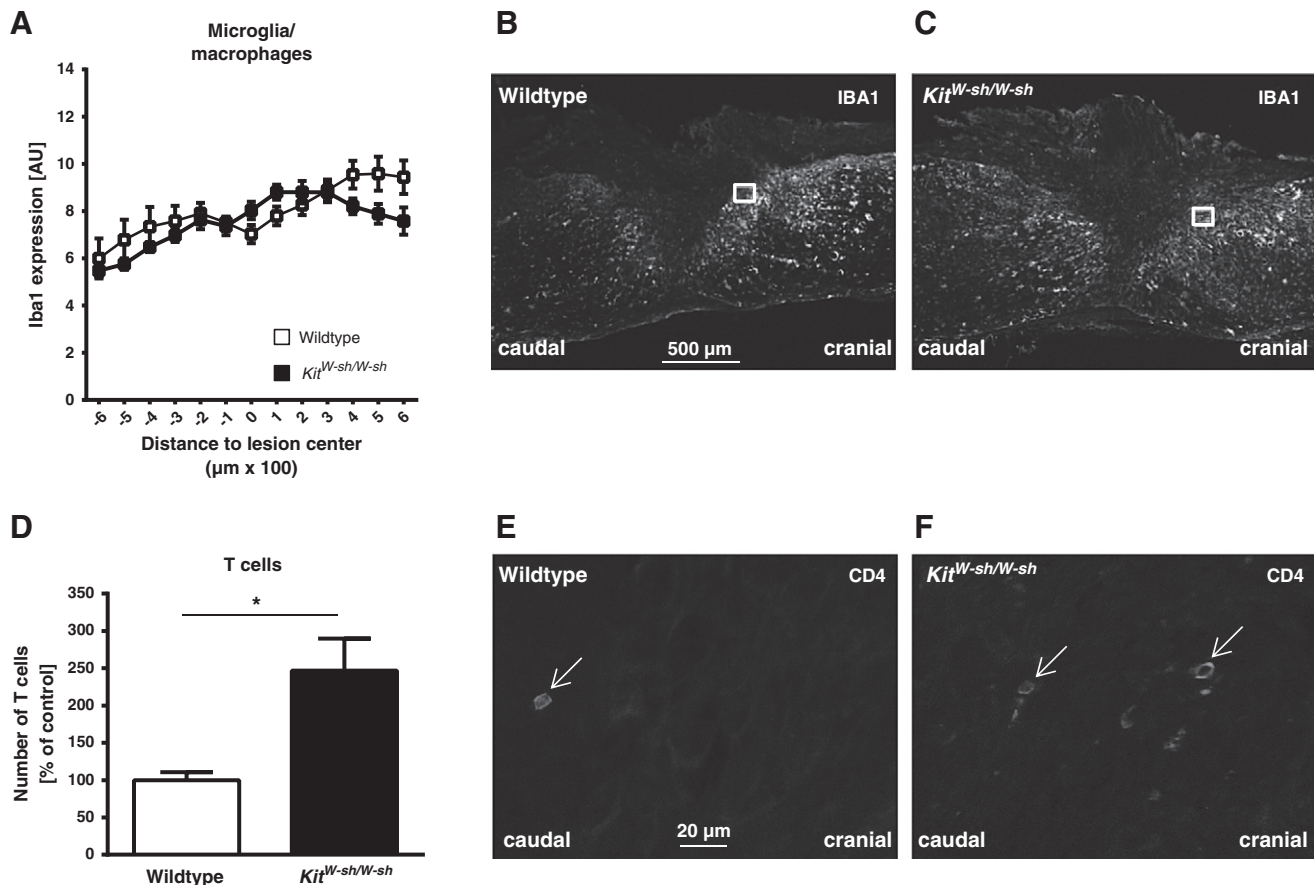


Fig. 2. Increased T cell infiltration in MC-deficient *Kit^{W-sh/W-sh}* mice after SCI. Quantification of Iba-1 expression just below the lesion site showed no difference in microglia/macrophage reaction between the MC-deficient *Kit^{W-sh/W-sh}* and WT mice (A). Representative pictures of the spinal cord sections including the injury epicenter, of WT mice and MC-deficient mice, respectively (B, C). Significantly more CD4+ T cells are present in the spinal cord sections of the MC-deficient mice, compared to control mice, 3 weeks after SCI (D). Boxed regions in B and C (Iba-1 staining) are shown in E and F (CD4 staining) to localize the T cells in the spinal cord. The arrows in pictures E–F indicate CD4+ T cells. Scale bars: B–C = 500 μm and E–F = 20 μm. Data represent mean ± SEM (expressed as percentage of control in panel D). **p* < 0.05. *n* = 8/group. Two independent experiments.

(Pineau and Lacroix, 2007) using in situ hybridization, no second mRNA peaks were observed for TNF-α and IL-1β mRNA in our analysis (Figs. 3C and E). IL-13 results were inconsistent and levels of IL-4 were very low and mostly undetectable (data not shown).

Analysis of both local (spinal cord lysate) as well as systemic (serum) protein levels revealed peak IL-6 protein levels 6 h after SCI, both locally (Fig. 4A) and systemically (Fig. 4F), followed by a decrease to basal levels around 4 days post injury. Locally, this increase was specifically found after T-cut hemisection SCI and not after laminectomy, while a systemic increase in IL-6 levels is seen already after laminectomy alone (Fig. 4A). MCP-1 protein levels were significantly increased in the spinal cord after SCI both in the acute phase (6 h and 2 days) as well as at 4 days and 7 days after SCI compared to protein levels in the uninjured and laminectomy (sham) mice (Fig. 4B). Systemically, a significantly higher level of MCP-1 was found at 2 days compared to 4 days after SCI (Fig. 4G). IL-1β results were inconsistent in serum and tissue samples (data not shown). Although TNF-α mRNA levels increased substantially in the spinal cord after lesion (Fig. 3C), surprisingly the opposite was found on the protein level: TNF-α protein levels significantly decreased at almost all time points measured after SCI, both in spinal cord (Fig. 4C) as well as in serum samples (Fig. 4H). In laminectomy (sham) mice however, local and systemic TNF-α levels did not show any significant difference when compared to uninjured mice at any time point investigated. Also, for the anti-inflammatory cytokine IL-10, the increased mRNA levels observed in the acute phase after SCI (Fig. 3D) are in sharp contrast with the protein levels of IL-10 in the spinal cord (data not shown), which were unaffected at almost all time points after SCI. Finally, IL-4 levels decreased locally in the acute phase to

reach again basal levels in the early stage of the chronic remodeling phase (28 days, Fig. 4D).

Taking all these data together, it became clear that the most important changes in the cytokine profiles occur in the acute phase (1 h, 6 h and 2 days) after SCI. Hence, this time-window was the focus in the following experiments.

*MCP-1 and IL-6 levels are increased in MC-deficient *Kit^{W-sh/W-sh}* mice compared to WT controls after injury*

Local MCP-1 (Fig. 5A), TNF-α (Fig. 5B), IL-10 (Fig. 5C) and IL-13 (Fig. 5D) protein levels were increased compared to uninjured mice 6 h after SCI. However, we need to emphasize that only MCP-1 was significantly increased compared to basal levels in uninjured mice. Systemically, only IL-6 protein levels were significantly increased 6 h after SCI in MC-deficient *Kit^{W-sh/W-sh}* mice compared to the controls (Fig. 5E). A slight tendency towards increased MCP-1, TNF-α and IL-10 could also be observed systemically and the same trend was visible in local IL-6 protein levels in MC-deficient *Kit^{W-sh/W-sh}* mice (data not shown). IL-1β results were inconsistent in serum samples and local levels of IL-4 were below detection limit (data not shown).

mMCP4-deficiency results in a decreased functional recovery and increased cytokine levels after SCI

As a next step, we addressed the question whether MCs restrict the inflammatory process and degeneration after CNS trauma through the release of proteases, which in turn degrade pro-inflammatory as well

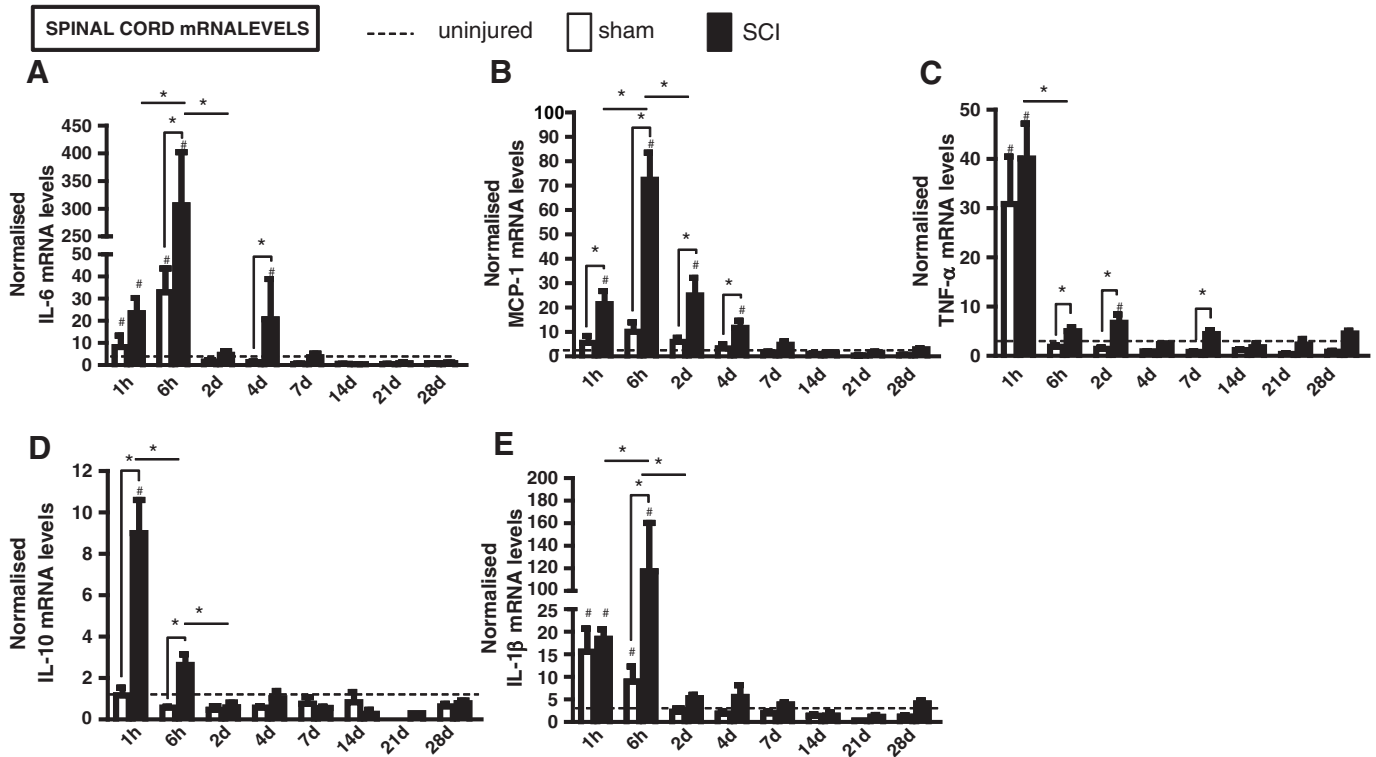


Fig. 3. Peak mRNA levels of pro- and anti-inflammatory cytokines in the acute phase after SCI. Normalized mRNA levels of pro- and anti-inflammatory cytokines in the spinal cord at selected time points after SCI are shown (A–E). Peak levels of TNF-α (C) and IL-10 mRNA (D) 1 h after surgery. Six hours after SCI, IL-6 (A), MCP-1 (B) and IL-1β (E) mRNA levels reached a peak, and were significantly higher compared to the sham-operated and uninjured mice. * $p < 0.05$ compared to previous/next time point (indicated by line), # $p < 0.05$ compared to sham-operated mice and # $p < 0.05$ compared to uninjured mice. $n = 3$ –5/time point.

as chemotactic factors. To this end, mMCP4 (an MC-specific chymase) knockout mice (mMCP4^{-/-}) were subjected to SCI and BMS analysis was performed daily. Functional recovery was decreased from day 7 onwards in mMCP4^{-/-} mice, when compared to their corresponding controls (Fig. 6A). In addition, a significant increase in lesion size (Figs. 6B, C, F) and demyelinated area (Figs. 6D, E, G) was observed in mMCP4^{-/-} mice. No differences in astrogliosis and microglia/macrophage infiltration were observed between mMCP4^{-/-} mice and their controls. The level of GFAP expression (Fig. 6H) and Iba1 expression (Fig. 6I) was unchanged. Analysis of CD4 expression at the lesion site revealed a significant reduction in T cell infiltration in mMCP4^{-/-} mice after SCI, compared to WT mice (Fig. 6J).

Local IL-6 (Fig. 7A) and MCP-1 (Fig. 7B) protein levels of mMCP4^{-/-} mice were significantly increased compared to protein levels in WT mice 1 h, 6 h and 2 days after SCI. Local IL-13 protein levels of mMCP4^{-/-} mice were significantly increased compared to protein levels in WT mice 1 h after SCI (Fig. 7C). Locally, levels of IL-4 were below detection limit and levels of TNF-α and IL-10 were unaffected (data not shown). Systemically, IL-6 (Fig. 7D) and MCP-1 (Fig. 7E) protein levels in mMCP4^{-/-} mice were significantly higher 1 h and 6 h after SCI compared to WT mice. Increased TNF-α (Fig. 7F) and IL-13 (Fig. 7H) protein levels 1 h, 6 h and 2 days after SCI in serum samples of mMCP4^{-/-} mice compared to WT mice were observed. IL-10 (Fig. 7G) protein levels in serum samples of mMCP4^{-/-} mice are significantly higher 6 h and 2 days after SCI compared to levels in WT mice. IL-4 protein levels in the serum were unaffected after SCI (data not shown).

MCP-1, IL-6 and IL-13 are substrates for mMCP4

To further clarify how mMCP4 may restrict the inflammatory process after SCI, an in vitro degradation assay was performed. Recombinant MCP-1, IL-6, TNF-α, IL-10, IL-13 as well as IL-1β protein were incubated for 6, 48 or 96 h in the presence of MC supernatant derived

from BMCMC either obtained from C57BL/6 mice or mMCP4^{-/-} mice (BMCMB₆ or BMCMB_{mMCP4^{-/-}}). None of the above cytokines displayed any cleavage following incubation for 6 h with either BMCMB₆ or BMCMB_{mMCP4^{-/-}} supernatant (data not shown). Incubation of MCP-1, IL-6, TNF-α, IL-10 as well as IL-13 for 48 h with BMCMB₆ supernatant resulted in cleavage of these cytokines (Fig. 8A, upper panel arrows). Similar results were obtained with MC supernatant derived from peritoneal derived cultured MCs (data not shown). However, when MCP-1, IL-6 and IL-13 were incubated with BMCMB_{mMCP4^{-/-}} supernatant, this cleavage was decreased, indicating that mMCP4 is at least in part responsible for this cleavage. Intensity analysis of the corresponding bands confirmed these findings (Figs. 8B–G). The cleavage of MCP-1 and IL-13 was even more pronounced after 96 h of incubation (Fig. 8A, lower panel, Figs. 8B and F).

Discussion

The role of MCs in neuroinflammatory diseases such as stroke and MS is complex. Depending on the animal model, MCs may exert beneficial or detrimental effects or may even be dispensable (Bennett et al., 2009; Lindsberg et al., 2010; Piconese et al., 2011). In the present study, we found that functional recovery is significantly reduced in MC-deficient *Kit*^{W-sh/W-sh} mice and *Kit*^{W/Kit}^{W-v} mice after SCI compared to WT mice. Further histological analyses of the *Kit*^{W-sh/W-sh} mice revealed significantly increased astrogliosis and an extensive T cell infiltration. In addition, we addressed the question by which mechanism MCs may protect from spinal cord inflammation. A degradation assay revealed that selected cytokines (MCP-1, IL-6 and IL-13) which are upregulated in both MC-deficient mice and mMCP4^{-/-} mice, are substrates of the MC protease mMCP4.

In the present study we investigated the role of MCs in an in vivo model of mechanical CNS trauma, namely SCI with a clear and measurable functional outcome. We decided to use a well-established model

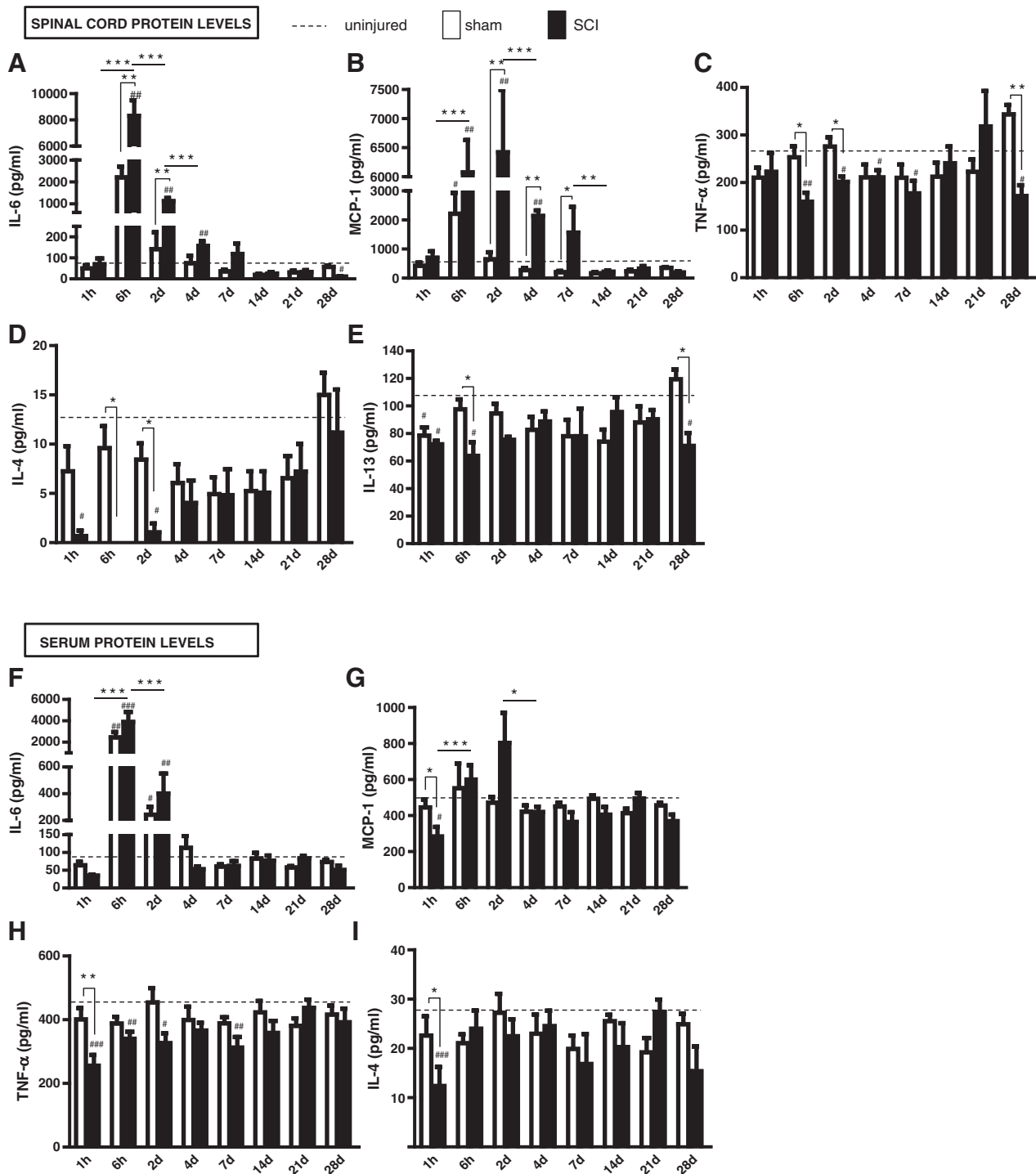


Fig. 4. Peak protein levels of IL-6 and MCP-1 after SCI. Significantly higher protein levels are noted in the supernatants of spinal cord homogenates for IL-6 (A), 6 h (peak) and 2 days after SCI compared to levels in uninjured and sham-operated mice, whereas MCP-1 (B) protein reach peak levels in the supernatants of spinal cord homogenates 2 days after SCI that are significantly different compared to uninjured and sham-operated mice. In contrast, TNF-α (C) protein levels significantly decrease 6 h and 2 days after SCI in the supernatants of spinal cord homogenates compared to uninjured and sham-operated mice, similar to what is found for the anti-inflammatory cytokines IL-4 (D) and IL-13 (E). Systemically, significantly higher protein levels are found in the serum for IL-6 (F), 6 hours after SCI compared to uninjured mice. MCP-1 (G), TNF-α (H) as well as IL-4 (I) show decreased protein levels 1 h after SCI compared to uninjured and sham-operated mice. * $p < 0.05$, ** $p < 0.01$ and *** $p < 0.001$ compared to previous/next time point (indicated by line); * $p < 0.05$ and ** $p < 0.01$ compared to sham-operated mice; # $p < 0.05$, ## $p < 0.01$ and ### $p < 0.001$ compared to uninjured mice. $n = 5-12$ /time point. Three independent experiments.

of a T-cut hemisection injury (Tuszynski and Steward, 2012) in order to produce a very standardized lesion without spared fibers. Contusion injury models may be considered as being closer to the in vivo situation in patients, however, these models tend to show more variations of the lesion and also a considerable number of spared fibers. Functional analysis of the *Kit^{W-sh/W-sh}* mice after SCI revealed a significantly reduced

functional recovery in the BMS, which was associated with increased T cell infiltration and perilesional astrogliosis. Lesion size, demyelination and macrophage/microglia presence caudal to the lesion site, showed a slight trend towards increase in MC-deficient mice which did not reach statistical significance. Although T cells may have beneficial effects under certain experimental conditions, however, a dramatic

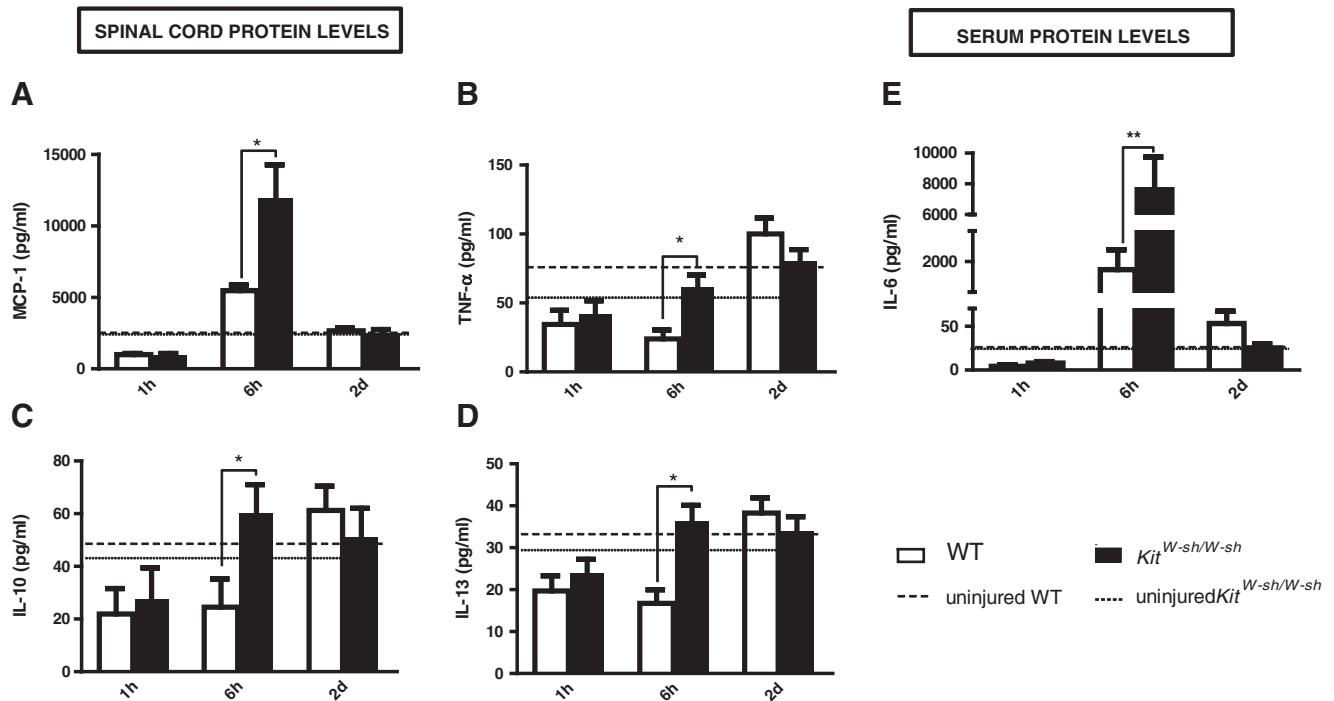


Fig. 5. Increased MCP-1, TNF- α , IL-10 and IL-13 protein levels in the supernatants of spinal cord homogenates and increased IL-6 protein levels in serum samples of *Kit^{W-sh/W-sh}* mice, 6 h after SCI compared to WT counterparts. In contrast to IL-6 and IL-1 β (data not shown), in the supernatants of spinal cord homogenates, protein levels of MCP-1 (A), TNF- α (B), IL-10 (C) and IL-13 (D) in *Kit^{W-sh/W-sh}* mice are significantly higher 6 h after SCI compared to WT mice. Systemically IL-6 (E) protein levels in *Kit^{W-sh/W-sh}* mice are significantly higher 6 h after SCI compared to WT mice. * $p < 0.05$; ** $p < 0.01$ compared to WT mice. $n = 6$ –24/time point. Three independent experiments.

accumulation of endogenous T cells three weeks after lesion should be considered detrimental (Hendrix and Nitsch, 2007). Similarly, astrogliosis is important as an early repair mechanism in the early phases after injury while it may substantially impair recovery in later phases (Fitch and Silver, 2008). Thus, the combination of increased T cell infiltration and increased astrogliosis three weeks after lesion in the subacute to early chronic phase may explain – at least in part – the reduced functional outcome in MC- and MC protease deficient mice. In a parallel study, we demonstrated, by using an entorhinal cortex lesion model, an increased exacerbated brain inflammation after mechanical brain injury in *Kit^W/Kit^{W-v}* and *Kit^{W-sh/W-sh}* mice, suggesting a protective role for MCs in brain trauma (Hendrix et al., 2013). In mMCP4-deficient mice we also found a significantly reduced locomotor score combined with a significant increase in lesion size and demyelinated area.

In both MC-deficient mouse lines and in two distinct models of CNS injury, there was good evidence that MCs play a key role in functional recovery after CNS trauma. However, it must be kept in mind that not all effects seen in *Kit^W/Kit^{W-v}* and *Kit^{W-sh/W-sh}* mice may be a result of MC-deficiency since some *kit* effects appear to be independent of MCs (Feyerabend et al., 2011). *Kit^W/Kit^{W-v}* mice are sterile, neutropenic and anemic and have impaired melanogenesis (Galli and Kitamura, 1987). They also show impairments in lymphocyte development, gut motility and pain sensation. In contrast, *Kit^{W-sh/W-sh}* mice are fertile and not anemic, however, they have neutrophilia and defects in skin pigmentation, exhibit an anxiety-like phenotype and show a time-dependent loss in MCs (Grimbaldeston et al., 2005; Nautiyal et al., 2008). This means that they are profoundly MC-deficient in all examined tissues except the skin, where age-dependent reduction in MC density occurs during the first 12 weeks of life. To control for MC-independent effects, MCs can be reconstituted to MC-deficient mice in order to abolish the effects induced by the absence of MCs. Extensive pilot experiments, however, revealed that MC reconstitution lead only to a partial redistribution of MCs in the meninges, but not in the CNS parenchyma (S. Hendrix, unpublished observation). Similarly, in a study using green

fluorescent protein-expressing BMCMC for MC reconstitution in *Kit^W/Kit^{W-v}* mice, MC populations were not restored in several organs such as lymph nodes, heart, brain and spinal cord (Tanzola et al., 2003). Therefore, in our opinion reconstitution experiments are not ideal to distinguish between MC-dependent and independent effects in the CNS.

In order to further investigate the immunological mechanism of the decreased functional outcome, we analyzed mRNA and protein levels of selected inflammation-associated cytokines at key time points after SCI. The selected cytokines were chosen because they are well-known to play a role in SCI and show significant changes of expression after SCI (Donnelly and Popovich, 2008; Pineau and Lacroix, 2007). We found peak mRNA levels of TNF- α , MCP-1, IL-1 β , IL-6, and IL-10 in the spinal cord tissue following the first 1 and 6 h after injury. In contrast, on the protein level, only MCP-1 and IL-6 peaks were detectable at 6 h and 2 days after lesion. The discrepancy seen between mRNA and protein levels of inflammatory factors is a well-known phenomenon, for example, as seen with TNF- α and IL-10. TNF- α expression is regulated transcriptionally as well as post-transcriptionally (Anderson et al., 2004; Jacob and Tashman, 1993; Means et al., 2000). Post transcriptional control of TNF- α expression requires the AU-rich elements (ARE) in the 3' untranslated region (UTR), which are important in controlling message stability and translational activation (Kontoyiannis et al., 1999). Individual ARE-binding proteins can promote or inhibit the expression of TNF- α . The best characterized examples of inhibitory ARE-binding proteins for TNF- α are tristetrapolin (TTP), an unusual zinc finger protein whose expression is induced by both LPS and TNF- α itself (Carballo and Blackshear, 2001; Carballo et al., 1998; Lai et al., 2000), as well as T cell intracellular antigen-1 (TIA-1) (Phillips et al., 2004; Piecyk et al., 2000) and TIA-1-related (TIAR) (Gueydan et al., 1999). Also for IL-10, it is well described that the availability of its mRNA levels and the amount of detectable protein vary significantly. This post-transcriptional control also depends on ARE-rich elements in the 3'UTR of mouse IL-10 (Powell et al., 2000). A growing class of non-coding RNAs called microRNAs (miRNAs), is involved in post-transcriptional regulation of genes like IL-

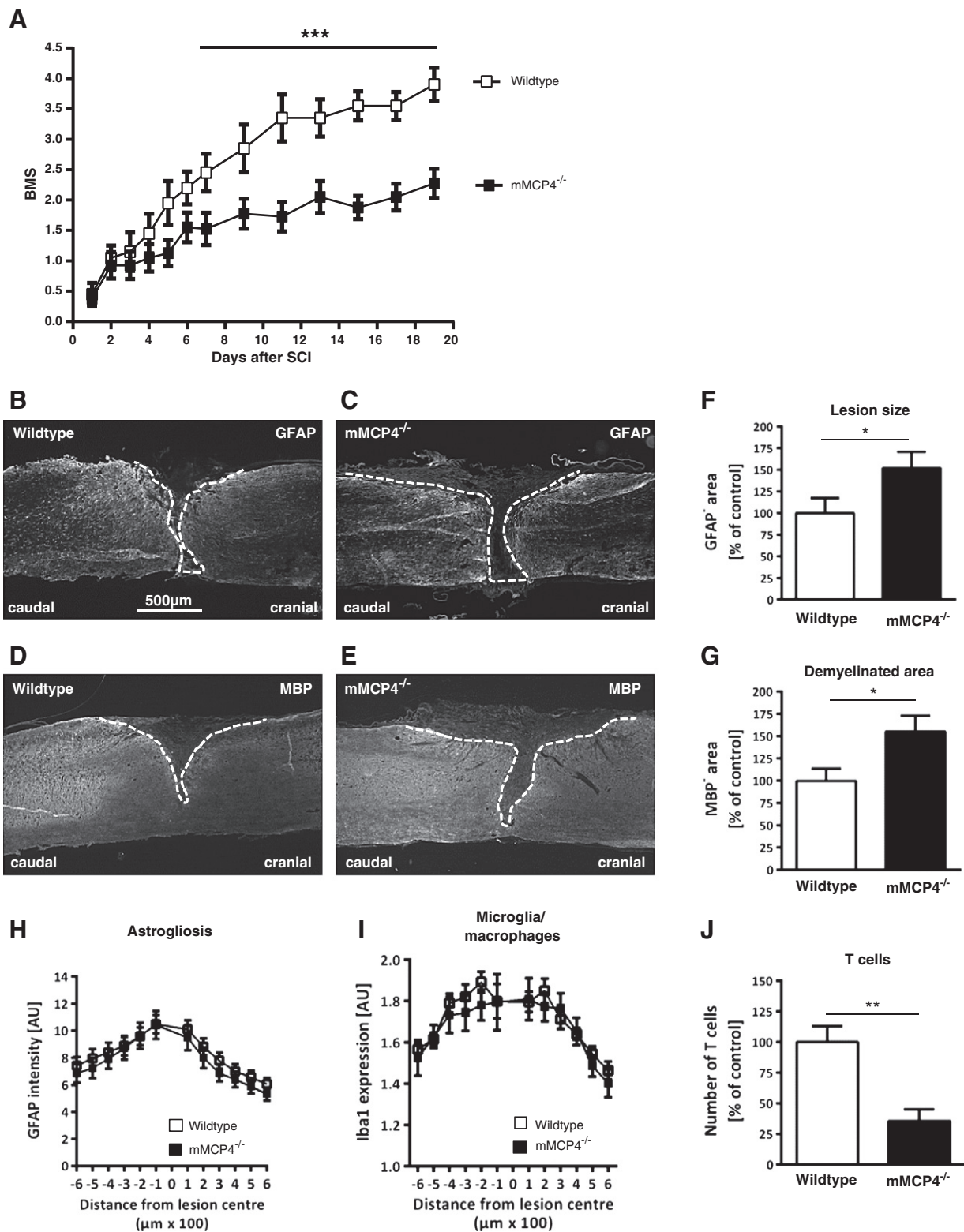


Fig. 6. Decreased functional outcome, increased lesion size and demyelinated area in mMCP4^{-/-} mice compared to WT after SCI. The deficiency of mMCP4 in mMCP4^{-/-} mice results in a significantly decreased BMS score after SCI (A). *** p < 0.001. n = 10–18/group. Two independent experiments. Representative photomicrographs of spinal cord sections showing the injury epicenter of WT mice (B, D) and mMCP4^{-/-} mice (C, E). Sections were stained for GFAP (B, C) and MBP (D, E) to determine the lesion size (F) and the demyelinated area (G), respectively. Lesion size and demyelinated area were determined by quantifying the GFAP-negative area and MBP-negative area, respectively (delineated with a dotted line). Image analysis revealed a significantly increased lesion size (F) and demyelinated (G) area in mMCP4^{-/-} mice, compared to WT mice. Quantification of GFAP expression and Iba-1 expression at the lesion site showed no difference in astrogliosis and in microglia/macrophage reaction between mMCP4^{-/-} and WT mice (H, I). A significantly decreased number of T cells was found in mMCP4^{-/-} mice compared to WT mice after SCI at the lesion area (J). Scale bars: B–E = 500 μm. Data represent mean ± SEM (expressed as percentage of control in panel F, G and J). *p < 0.05, **p < 0.01. n = 7–10/group. Two independent experiments.

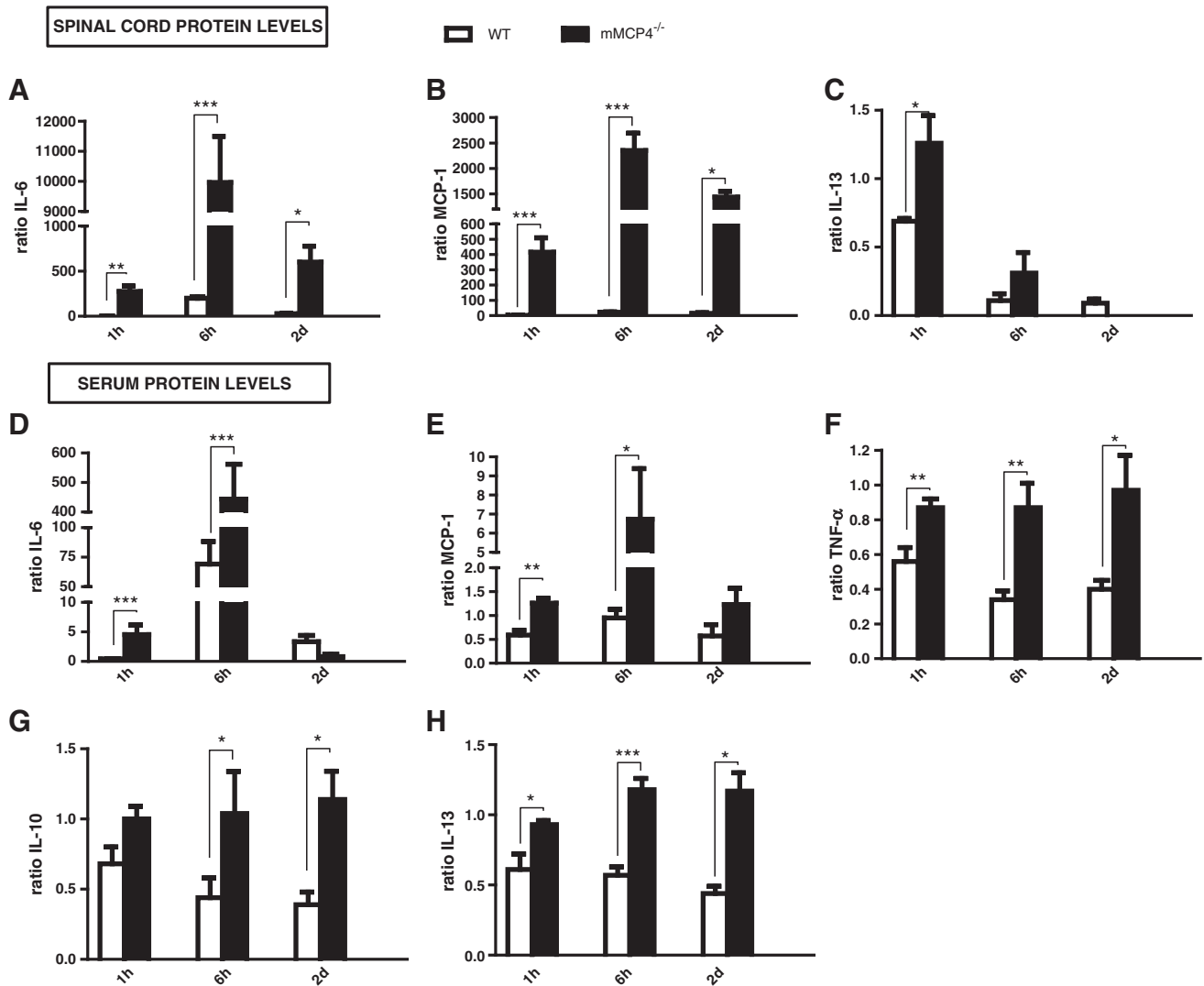


Fig. 7. Increased protein levels of MCP-1, IL-6 and IL-13 in spinal cord homogenates and serum samples of mMCP4^{-/-} mice after SCI, compared to WT mice. Since cytokine levels in uninjured WT mice are different from those in uninjured mMCP4^{-/-} mice, cytokine levels are expressed as a ratio of injured to uninjured mice for WT mice and mMCP4^{-/-} mice, respectively. Based on this ratio, IL-6 (A) and MCP-1 (B) protein levels in the supernatants of spinal cord homogenates in mMCP4^{-/-} mice are significantly higher 1 h, 6 h and 2 days after SCI as compared to WT mice. IL-13 protein levels in spinal cord homogenates in mMCP4^{-/-} mice are significantly higher 1 h after SCI compared to WT mice (C). IL-6 (D) and MCP-1 (E) protein levels in serum samples of mMCP4^{-/-} mice are significantly higher 1 h and 6 h after SCI compared to WT mice. Increased TNF-α (F) and IL-13 (H) protein levels 1 h, 6 h and 2 days after SCI in serum samples of mMCP4^{-/-} mice are shown compared to WT mice. IL-10 protein levels in serum samples of mMCP4^{-/-} mice are significantly higher 6 h and 2 days after SCI compared to WT mice (G). *p < 0.05, **p < 0.01 and ***p < 0.001. n = 3–10/time point. Two independent experiments.

10, such as has-miR-106a (Bartel, 2004; Sharma et al., 2009). Further analyses revealed that IL-6 levels in the serum and MCP-1, TNF-α, IL-10 and IL-13 protein levels in the spinal cord of MC-deficient *Kit^{W-sh/W-sh}* mice are significantly increased compared to WT controls in the acute phase after SCI. The significant changes in cytokine levels reported here are not subtle (around 200% increase or more), suggesting biological relevance. These findings indicate a substantial change in the local immune milieu, which on the one hand is composed of IL-10 and proves beneficial after SCI (Brewer et al., 1999; Zhou et al., 2009) and on the other, contains MCP-1 and TNF-α which are rather detrimental (Esposito and Cuzzocrea, 2011; Gao and Ji, 2010). It may appear puzzling that significant differences of cytokine levels between MC-deficient mice and WT mice appear early while behavioral differences become detectable around day 7 after SCI. However, it is important to note that functional impairment before day 7 cannot be dramatic because the WT mice still have a very low BMS score (nearly zero) during the first week.

Since there is some indication that MC proteases may have protective effects in other contexts (Caughy, 2011; Hendrix et al., 2013; Pejler et al., 2010), we addressed the question whether the absence of MC proteases may be responsible for increased cytokine levels and CNS inflammation in MC-deficient mice. Consistently, absence of mMCP4 during and after SCI in mMCP4-deficient mice leads to decreased functional recovery similar to MC-deficiency in *Kit^{W-sh/W-sh}* mice. These data suggest that mMCP4-deficiency may be sufficient to reproduce the functional impairment seen in MC-deficient mice.

As a next step, we demonstrated in a degradation assay that BMCM supernatant cleaves recombinant MCP-1, IL-6, TNF-α, IL-10 and IL-13. This effect was completely abolished for MCP-1, IL-6 and IL-13 when supernatant derived from mMCP4-deficient mice was used, indicating that these cytokines are substrates for mMCP4. This is in line with the finding that skin MCs are able to degrade TNF-α, IL-6, and IL-13 (Zhao et al., 2005). The partial cleavage of TNF-α and IL-10 by mMCP4-

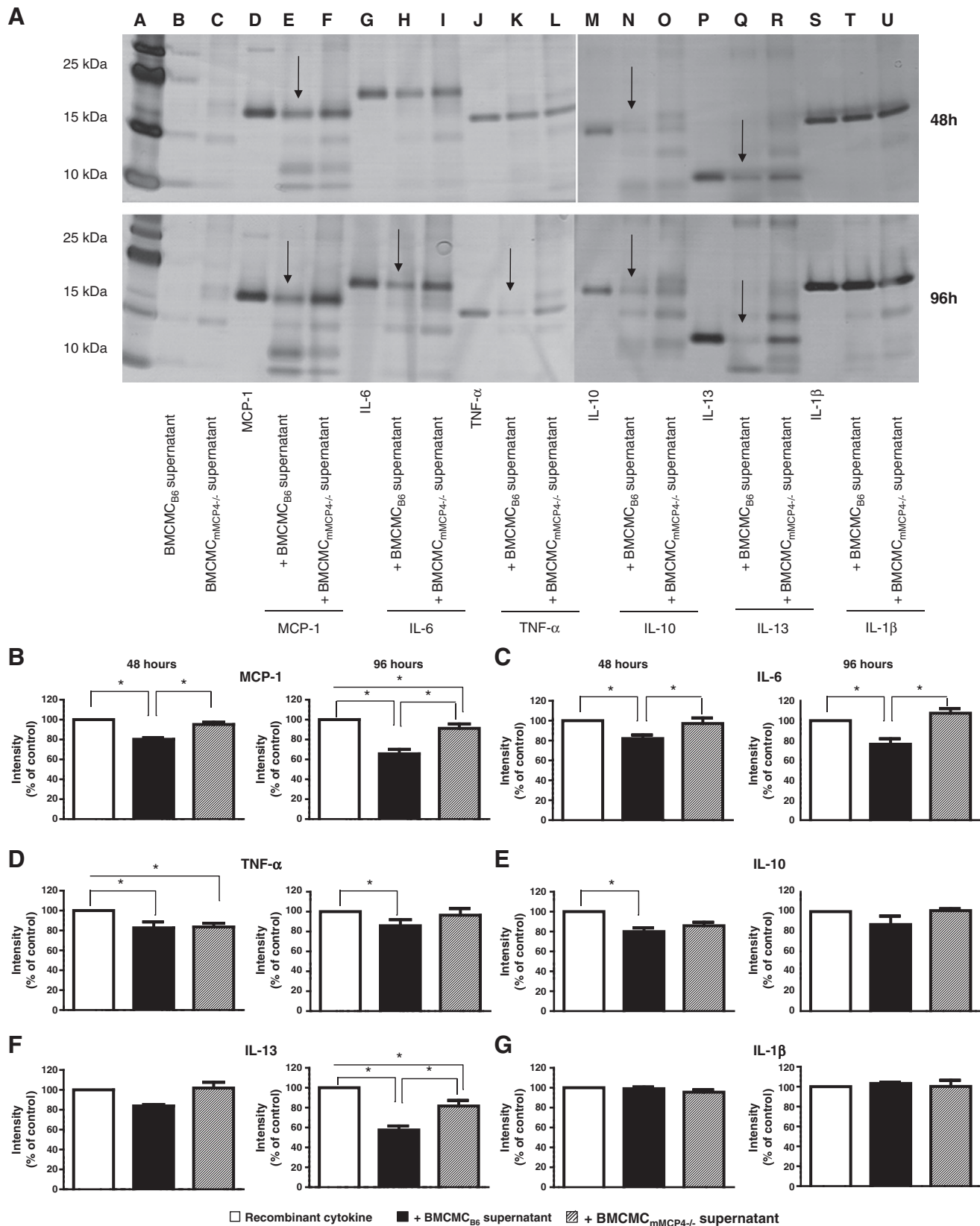


Fig. 8. MMCP4 cleaves MCP-1, IL-6 and IL-13. Incubation of recombinant MCP-1, IL-6 or IL-13 with supernatant from BMCMB_{mMCP4-/-} (lane F, I, L and R) resulted in a decreased cleaving of these cytokines compared to incubation with supernatant from BMCMB_{B6} (lane E, H, K and Q) both after 48 h (upper panel) and 96 h (lower panel) of incubation (A). Lane A = protein ladder. Intensity analysis was performed using ImageJ. Both 48 and 96 hour incubations of recombinant MCP-1 (B), IL-6 (C), IL-10 (E) or IL-13 (F) with supernatant derived from BMCMB_{B6} resulted in a significantly decreased intensity, indicative for cleavage. This effect was abolished when cytokines were incubated with BMCMB_{mMCP4-/-} (B-G). **p* < 0.05. *n* = 3–4/condition. Three independent experiments.

deficient MC supernatant suggests that other MC proteases than mMCP4 are involved. Thus, all selected factors except IL-1 β are cleaved by the MC supernatant. IL-13, IL-6 and MCP-1 show an mMCP4-dependent cleavage, whereas IL-10 and TNF- α show an MC-dependent cleavage which is not or not completely mMCP4-dependent. These findings correlate well with the increase of all five factors (IL-10, TNF- α , IL-13, IL-6, MCP-1) in MC-deficient mice (Fig. 5), while the specific cleavage of IL-13, IL-6 and MCP-1 by mMCP4 correlates well with the local increase of these three cytokines seen in mMCP4-deficient mice (Fig. 7). Consistent with these cleavage data, the relative increase of MCP-1, IL-6 and IL-13 protein levels is dramatically higher in spinal cord samples from mMCP4^{-/-} mice after SCI, compared to WT mice. On the other hand, IL-10 and TNF- α levels show no substantial changes after SCI in the absence of mMCP4.

In these experiments we have calculated protein ratios as the baseline levels of these proteins are lower in the knockout mice. Thus, when compared to WT mice, the protein ratios clearly illustrate the profound increase of these factors in the spinal cord tissue of knockout mice. We consider this substantial increase to be of much higher biological relevance than the absolute cytokine levels. Although the inactivation of mMCP4 does not affect the storage of other MC proteases, the number of MCs or the MC morphology (Tchougounova et al., 2003), it cannot be excluded that mMCP4 regulates the expression/maturation of one or many other proteases, which cleave inflammatory mediators (Sun et al., 2009; Tchougounova et al., 2005). Because recombinant mMCP4 is not commercially available, further experiments were not yet possible.

Based on these data, it was tempting to hypothesize that increased levels of IL-6 and MCP-1 in MC-deficient mice may be the basis for the approximately 150% increase of T cell infiltration after SCI because IL-6 and MCP-1 are effective chemoattractant factors for T cells (Carr et al., 1994; Loetscher et al., 1994; McLoughlin et al., 2005; Meares et al., 2012; Weissenbach et al., 2004). This is not compensated for by IL-10 and IL-13, which are known to have pleiotropic effects. As discussed above, an extensive accumulation of endogenous T cells should be considered detrimental (Hendrix and Nitsch, 2007) and may explain – at least in part – the impaired motor performance in MC-deficient mice. However, in striking contrast to the MC-deficient mice, the number of infiltrating T cells was substantially reduced in mMCP4^{-/-} mice. This is also in contrast to the entorhinal cortex lesion model where we found a highly significant increase of T cell infiltration in mMCP4-deficient mice (Hendrix et al., 2013). These data strongly suggest that T cells are not the key players responsible for impaired functional and histological outcome in mMCP4-deficient mice after SCI. It is tempting to speculate that direct effects of cytokines on neurons and oligodendrocytes (Vidal et al., 2013) may be responsible for a reduced functional recovery following trauma to the spinal cord. MCs may also play a role in neuropathic pain: MC mediators such as TNF- α and histamine may sensitize nociceptors, and the MC-specific serine protease, tryptase, has been shown to trigger inflammatory hyperalgesia and nociceptive behavior in rats (reviewed in (Austin and Moalem-Taylor, 2010; McMahon et al., 2005; Watkins et al., 2007)). Therefore, future studies have to elucidate whether MCs and especially mMCP4 may influence the development of neuropathic pain after SCI. It appears puzzling that there is no significant difference in Iba-1 + cells between WT and MC-deficient mice after SCI, although MCP-1 is a potent chemoattractant for microglia/macrophages (Hinojosa et al., 2011). However, substantially increased levels of MCP-1 mRNA and protein levels were detected in the acute phase after injury with a peak at 6 h and 2 days, respectively, whereas Iba-1 levels were analyzed histologically three weeks after lesion. Thus, it cannot be excluded that there may have been an early peak of Iba-1 + cells which is not present anymore three weeks after injury.

Another potential approach to test MC-function may be the use of MC ‘stabilizers’ (agents that block MC degranulation following activation) (Galli and Tsai, 2008). One such drug is disodium cromoglycate.

However, the molecular targets of this drug are not restricted to MCs, as it can also influence the function of granulocytes and B cells (Norris, 1996). MC ‘stabilizers’ cannot be used to test our hypothesis that MC proteases dampen the inflammatory response after CNS trauma, because the secretion of proinflammatory factors from MC would also be blocked by this compound. Local application of a chymase inhibitor (chymostatin) did not change functional recovery after SCI (data not shown). Further experiments to test different administration methods and different concentrations are needed.

In summary, we show here for the first time that the absence of MCs can result in increased pathology and morbidity after SCI. We provide evidence that proteases secreted from MCs that degranulate after the injury, may be responsible for this protective effect by digesting inflammation-associated proteins. Finally, we show that the MC-specific chymase mMCP4 may account for most of these effects and that its absence results in impaired functional recovery after SCI. These data suggest a novel mechanism by which MCs and their proteases may protect the CNS from excessive pro-inflammatory cytokine levels and consecutive tissue damage after trauma.

Acknowledgments

This study was supported in part by grants from Deutsche Forschungsgemeinschaft (SPP1394) and from Fonds Wetenschappelijk Onderzoek – Vlaanderen (FWO) to SH (G.0389.12, G0A5813), to EL (1.2.703.10N) and LG (1.5.056.12N), and from Agentschap voor Innovatie door Wetenschap en Technologie (IWT) to TV. PV is a PhD student of the Transnational University Limburg. This work has benefited from the support of the COST ACTION BM1007 MAST CELLS AND BASOPHILS – TARGETS FOR INNOVATIVE THERAPIES.

References

- Anderson, P., et al., 2004. Post-transcriptional regulation of proinflammatory proteins. *J. Leukoc. Biol.* 76, 42–47.
- Austin, P.J., Moalem-Taylor, G., 2010. The neuro-immune balance in neuropathic pain: involvement of inflammatory immune cells, immune-like glial cells and cytokines. *J. Neuroimmunol.* 229, 26–50.
- Bartel, D.P., 2004. MicroRNAs: genomics, biogenesis, mechanism, and function. *Cell* 116, 281–297.
- Bartholdi, D., Schwab, M.E., 1997. Expression of pro-inflammatory cytokine and chemokine mRNA upon experimental spinal cord injury in mouse: an in situ hybridization study. *Eur. J. Neurosci.* 9, 1422–1438.
- Basso, D.M., et al., 2006. Basso Mouse Scale for locomotion detects differences in recovery after spinal cord injury in five common mouse strains. *J. Neurotrauma* 23, 635–659.
- Beck, K.D., et al., 2010. Quantitative analysis of cellular inflammation after traumatic spinal cord injury: evidence for a multiphasic inflammatory response in the acute to chronic environment. *Brain* 133, 433–447.
- Bennett, J.L., et al., 2009. Bone marrow-derived mast cells accumulate in the central nervous system during inflammation but are dispensable for experimental autoimmune encephalomyelitis pathogenesis. *J. Immunol.* 182, 5507–5514.
- Brenner, T., et al., 1994. Mast cells in experimental allergic encephalomyelitis: characterization, distribution in the CNS and in vitro activation by myelin basic protein and neuropeptides. *J. Neurol. Sci.* 122, 210–213.
- Brewer, K.L., et al., 1999. Neuroprotective effects of interleukin-10 following excitotoxic spinal cord injury. *Exp. Neurol.* 159, 484–493.
- Brown, M.A., et al., 2002. Mechanisms underlying mast cell influence on EAE disease course. *Mol. Immunol.* 38, 1373–1378.
- Carballo, E., Blakeshear, P.J., 2001. Roles of tumor necrosis factor- α receptor subtypes in the pathogenesis of the tristetraprolin-deficiency syndrome. *Blood* 98, 2389–2395.
- Carballo, E., et al., 1998. Feedback inhibition of macrophage tumor necrosis factor- α production by tristetraprolin. *Science* 281, 1001–1005.
- Carr, M.W., et al., 1994. Monocyte chemoattractant protein 1 acts as a T-lymphocyte chemoattractant. *Proc. Natl. Acad. Sci. U. S. A.* 91, 3652–3656.
- Caughy, G.H., 2011. Mast cell proteases as protective and inflammatory mediators. *Adv. Exp. Med. Biol.* 716, 212–234.
- Donnelly, D.J., Popovich, P.G., 2008. Inflammation and its role in neuroprotection, axonal regeneration and functional recovery after spinal cord injury. *Exp. Neurol.* 209, 378–388.
- Dudek, A., et al., 2010. Immature mast cells exhibit rolling and adhesion to endothelial cells and subsequent diapedesis triggered by E- and P-selectin, VCAM-1 and PECAM-1. *Exp. Dermatol.* 19, 424–434.
- Esposito, E., Cuzzocrea, S., 2011. Anti-TNF therapy in the injured spinal cord. *Trends Pharmacol. Sci.* 32, 107–115.
- Feyerabend, T.B., et al., 2011. Cre-mediated cell ablation contests mast cell contribution in models of antibody- and T cell-mediated autoimmunity. *Immunity* 35, 832–844.

- Fitch, M.T., Silver, J., 2008. CNS injury, glial scars, and inflammation: Inhibitory extracellular matrices and regeneration failure. *Exp. Neurol.* 209, 294–301.
- Galli, S.J., Kitamura, Y., 1987. Genetically mast-cell-deficient W/W^v and Sl/Sld mice. Their value for the analysis of the roles of mast cells in biologic responses in vivo. *Am. J. Pathol.* 127, 191–198.
- Galli, S.J., Tsai, M., 2008. Mast cells: versatile regulators of inflammation, tissue remodeling, host defense and homeostasis. *J. Dermatol. Sci.* 49, 7–19.
- Gao, Y.J., Ji, R.R., 2010. Chemokines, neuronal-glial interactions, and central processing of neuropathic pain. *Pharmacol. Ther.* 126, 56–68.
- Grimbaldeston, M.A., et al., 2005. Mast cell-deficient W-sash c-kit mutant Kit W-sh/W-sh mice as a model for investigating mast cell biology in vivo. *Am. J. Pathol.* 167, 835–848.
- Gueydan, C., et al., 1999. Identification of TIAR as a protein binding to the translational regulatory AU-rich element of tumor necrosis factor alpha mRNA. *J. Biol. Chem.* 274, 2322–2326.
- Hendrix, S., Nitsch, R., 2007. The role of T helper cells in neuroprotection and regeneration. *J. Neuroimmunol.* 184, 100–112.
- Hendrix, S., et al., 2013. Mast cells protect from post-traumatic brain inflammation by the mast cell-specific chymase mouse mast cell protease-4. *FASEB J.* 27, 920–929.
- Henz, B.M., et al., 2001. Mast cells as initiators of immunity and host defense. *Exp. Dermatol.* 10, 1–10.
- Hinojosa, A.E., et al., 2011. CCL2/MCP-1 modulation of microglial activation and proliferation. *J. Neuroinflammation* 8, 77.
- Jacob, C.O., Tashman, N.B., 1993. Disruption in the AU motif of the mouse TNF-alpha 3' UTR correlates with reduced TNF production by macrophages in vitro. *Nucleic Acids Res.* 21, 2761–2766.
- Jin, Y., et al., 2009. Mast cells are early responders after hypoxia-ischemia in immature rat brain. *Stroke* 40, 3107–3112.
- Kil, K., et al., 1999. T cell responses to myelin basic protein in patients with spinal cord injury and multiple sclerosis. *J. Neuroimmunol.* 98, 201–207.
- Kontoyiannis, D., et al., 1999. Impaired on/off regulation of TNF biosynthesis in mice lacking TNF AU-rich elements: implications for joint and gut-associated immunopathologies. *Immunity* 10, 387–398.
- Lai, W.S., et al., 2000. Interactions of CCHZ zinc finger proteins with mRNA. Binding of tristetraprolin-related zinc finger proteins to AU-rich elements and destabilization of mRNA. *J. Biol. Chem.* 275, 17827–17837.
- Li, H., et al., 2011. Kit (W-sh) mice develop earlier and more severe experimental autoimmune encephalomyelitis due to absence of immune suppression. *J. Immunol.* 187, 274–282.
- Lindsberg, P.J., et al., 2010. Mast cells as early responders in the regulation of acute blood-brain barrier changes after cerebral ischemia and hemorrhage. *J. Cereb. Blood Flow Metab.* 30, 689–702.
- Loetscher, P., et al., 1994. Monocyte chemotactic proteins MCP-1, MCP-2, and MCP-3 are major attractants for human CD4⁺ and CD8⁺ T lymphocytes. *FASEB J.* 8, 1055–1060.
- Loske, P., et al., 2012. Minimal essential length of *Clostridium botulinum* C3 peptides to enhance neuronal regenerative growth and connectivity in a non-enzymatic mode. *J. Neurochem.* 120, 1084–1096.
- Marshall, J.S., 2004. Mast-cell responses to pathogens. *Nat. Rev. Immunol.* 4, 787–799.
- McLoughlin, R.M., et al., 2005. IL-6 trans-signaling via STAT3 directs T cell infiltration in acute inflammation. *Proc. Natl. Acad. Sci. U. S. A.* 102, 9589–9594.
- McMahon, S.B., et al., 2005. Immune and glial cell factors as pain mediators and modulators. *Exp. Neurol.* 192, 444–462.
- Means, T.K., et al., 2000. Activation of TNF-alpha transcription utilizes distinct MAP kinase pathways in different macrophage populations. *J. Leukoc. Biol.* 67, 885–893.
- Meares, G.P., et al., 2012. Regulation of CCL20 expression in astrocytes by IL-6 and IL-17. *Glia* 60, 771–781.
- Nautiyal, K.M., et al., 2008. Brain mast cells link the immune system to anxiety-like behavior. *Proc. Natl. Acad. Sci. U. S. A.* 105, 18053–18057.
- Nelissen, S., et al., 2013. The role of mast cells in neuroinflammation. *Acta Neuropathol.* 125, 637–650.
- Norris, A.A., 1996. Pharmacology of sodium cromoglycate. *Clin. Exp. Allergy* 26 (Suppl. 4), 5–7.
- Pan, J.Z., et al., 2002. Cytokine activity contributes to induction of inflammatory cytokine mRNAs in spinal cord following contusion. *J. Neurosci. Res.* 68, 315–322.
- Pejler, G., et al., 2010. Mast cell proteases: multifaceted regulators of inflammatory disease. *Blood* 115, 4981–4990.
- Phillips, K., et al., 2004. Arthritis suppressor genes TIA-1 and TTP dampen the expression of tumor necrosis factor alpha, cyclooxygenase 2, and inflammatory arthritis. *Proc. Natl. Acad. Sci. U. S. A.* 101, 2011–2016.
- Piconese, S., et al., 2011. Exacerbated experimental autoimmune encephalomyelitis in mast-cell-deficient Kit W-sh/W-sh mice. *Lab. Invest.* 91, 627–641.
- Piecyk, M., et al., 2000. TIA-1 is a translational silencer that selectively regulates the expression of TNF-alpha. *EMBO J.* 19, 4154–4163.
- Pineau, I., Lacroix, S., 2007. Proinflammatory cytokine synthesis in the injured mouse spinal cord: multiphasic expression pattern and identification of the cell types involved. *J. Comp. Neurol.* 500, 267–285.
- Powell, M.J., et al., 2000. Posttranscriptional regulation of IL-10 gene expression through sequences in the 3'-untranslated region. *J. Immunol.* 165, 292–296.
- Robbie-Ryan, M., et al., 2003. Cutting edge: both activating and inhibitory Fc receptors expressed on mast cells regulate experimental allergic encephalomyelitis disease severity. *J. Immunol.* 170, 1630–1634.
- Secor, V.H., et al., 2000. Mast cells are essential for early onset and severe disease in a murine model of multiple sclerosis. *J. Exp. Med.* 191, 813–822.
- Sharma, A., et al., 2009. Posttranscriptional regulation of interleukin-10 expression by hsa-miR-106a. *Proc. Natl. Acad. Sci. U. S. A.* 106, 5761–5766.
- Skaper, S.D., et al., 1996. Mast cell activation causes delayed neurodegeneration in mixed hippocampal cultures via the nitric oxide pathway. *J. Neurochem.* 66, 1157–1166.
- Skaper, S.D., et al., 2001. Potentiation by histamine of synaptically mediated excitotoxicity in cultured hippocampal neurons: a possible role for mast cells. *J. Neurochem.* 76, 47–55.
- Strbian, D., et al., 2006. Cerebral mast cells regulate early ischemic brain swelling and neurophil accumulation. *J. Cereb. Blood Flow Metab.* 26, 605–612.
- Strbian, D., et al., 2007. Mast cell blocking reduces brain edema and hematoma volume and improves outcome after experimental intracerebral hemorrhage. *J. Cereb. Blood Flow Metab.* 27, 795–802.
- Strbian, D., et al., 2009. An emerging role of mast cells in cerebral ischemia and hemorrhage. *Ann. Med.* 41, 438–450.
- Streit, W.J., et al., 1998. Cytokine mRNA profiles in contused spinal cord and axotomized facial nucleus suggest a beneficial role for inflammation and gliosis. *Exp. Neurol.* 152, 74–87.
- Sun, J., et al., 2009. Critical role of mast cell chymase in mouse abdominal aortic aneurysm formation. *Circulation* 120, 973–982.
- Tanzola, M.B., et al., 2003. Mast cells exert effects outside the central nervous system to influence experimental allergic encephalomyelitis disease course. *J. Immunol.* 171, 4385–4391.
- Tchougounova, E., et al., 2003. The chymase, mouse mast cell protease 4, constitutes the major chymotrypsin-like activity in peritoneum and ear tissue. A role for mouse mast cell protease 4 in thrombin regulation and fibronectin turnover. *J. Exp. Med.* 198, 423–431.
- Tchougounova, E., et al., 2005. A key role for mast cell chymase in the activation of pro-matrix metalloproteinase-9 and pro-matrix metalloproteinase-2. *J. Biol. Chem.* 280, 9291–9296.
- Tuszynski, M.H., Steward, O., 2012. Concepts and methods for the study of axonal regeneration in the CNS. *Neuron* 74, 777–791.
- Vidal, P.M., et al., 2013. The role of “anti-inflammatory” cytokines in axon regeneration. *Cytokine Growth Factor Rev.* 24, 1–12.
- Watkins, L.R., et al., 2007. “Listening” and “talking” to neurons: implications of immune activation for pain control and increasing the efficacy of opioids. *Brain Res. Rev.* 56, 148–169.
- Weissenbach, M., et al., 2004. Interleukin-6 is a direct mediator of T cell migration. *Eur. J. Immunol.* 34, 2895–2906.
- Zappulla, J.P., et al., 2002. Mast cells: new targets for multiple sclerosis therapy? *J. Neuroimmunol.* 131, 5–20.
- Zhao, W., et al., 2005. Cytokine production by skin-derived mast cells: endogenous proteases are responsible for degradation of cytokines. *J. Immunol.* 175, 2635–2642.
- Zhou, Z., et al., 2009. IL-10 promotes neuronal survival following spinal cord injury. *Exp. Neurol.* 220, 183–190.